



Seemingly Unlimited Lifetime Data Storage in Nanostructured Glass

Jingyu Zhang,^{*} Mindaugas Gecevičius, Martynas Beresna, and Peter G. Kazansky
Optoelectronics Research Centre, University of Southampton, Southampton SO17 1BJ, United Kingdom
(Received 1 November 2013; published 23 January 2014)

We demonstrate recording and retrieval of the digital document with a nearly unlimited lifetime. The recording process of multiplexed digital data was implemented by femtosecond laser nanostructuring of fused quartz. The storage allows unprecedented parameters including hundreds of terabytes per disc data capacity, thermal stability up to 1000 °C, and virtually unlimited lifetime at room temperature. We anticipate that this demonstration will open a new era of eternal data archiving.

DOI: 10.1103/PhysRevLett.112.033901

PACS numbers: 42.70.Ln, 42.50.Ct, 42.62.Cf, 78.20.Fm

Securely storing large amounts of information over even relatively short time scales of 100 years, comparable to the human memory span, is a challenging problem [1,2]. A general trend, defined in particular by the diffusion process, is a decrease in lifetime as the storage density increases. For example, a vast amount of data written by individual atoms can only be stored for 10 ps at room temperature [3,4]. The conventional optical data storage technology used for CDs and DVDs has reached capacities of hundreds of gigabits per square inch, but its lifetime is limited to several decades [5–7]. The major challenge is the lack of appropriate storage technology and a medium possessing the advantages of both high capacity and long lifetime.

The idea of optical recording based on femtosecond laser writing was first proposed and demonstrated in photopolymers [8]. Later, the virtue of high precision energy deposition attributed to ultrashort light pulses was explored for optical recording in the bulk of nonphotosensitive glass [9–11]. High capacity optical recording was also demonstrated by multiplexing new degrees of freedom including intensity, polarization, and wavelength by harnessing silver clusters embedded in glass [12] and plasmonic properties of gold or silver nanoparticles [13,14]. The method of data multiplexing is an alternative to holographic data storage [15], which allows overcoming the capacity limit dictated by optical diffraction. More recently, polarization multiplexed writing was demonstrated by using self-assembled nanogratings produced by ultrafast laser writing in fused quartz [16–18], which is renowned for its high chemical stability and resistance. The nanograting, featuring 20 nm embedded structures, the smallest ever produced by light [19–22], is a structural modification which can resist high temperatures [23]. Despite several attempts to explain the physics of the peculiar self-organization process, the formation of these nanostructures still remains debatable [16,21,24]. On the macroscopic scale the self-assembled nanostructure behaves as a uniaxial optical crystal with negative birefringence. The optical anisotropy, which results from the alignment of nanogratings, referred to as form birefringence, is of the same order of magnitude as

positive birefringence in crystalline quartz. The two independent parameters describing birefringence, the slow axis orientation (4th dimension) and strength of retardance (5th dimension, defined as a product of the birefringence and length of structure), were explored for the optical encoding of information in addition to three spatial coordinates [17]. The slow axis orientation and the retardance are independently manipulated by the polarization and intensity of the incident beam. However, conventional control using polarization optics turns the recording procedure of digital data into a slow serial process making real world applications unviable. Here we demonstrate the multilevel encoding of intensity and polarization states of light with self-assembled nanostructures and increase the data recording rate by 2 orders of magnitude. The first digital document optically encrypted into five dimensions is successfully retrieved by nondestructive quantitative birefringence measurements. The accelerated aging experiments demonstrate the unprecedented high stability of self-assembled nanostructures in silica glass.

Data recording experiments were performed with a Yb: KGW based femtosecond laser system (Pharos, Light Conversion Ltd.) operating at 1030 nm and delivering 6.3 μ J pulses at 200 kHz repetition rate and pulse duration tunable from 270 to 800 fs. Despite that a longer pulse duration can induce higher retardance (80 nm) [25], it also leads to higher stress accumulation and eventual material cracking [9]. As a result, the pulse duration was set to 280 fs. Three modification layers (Supplemental Material, movie 1 [26]) were inscribed with a femtosecond laser 130–170 μ m below the surface of a fused quartz (SiO_2 glass) sample by a 1.2 NA (60 \times) water immersion objective.

In the recording procedure, groups of birefringent dots were simultaneously imprinted at the designated depth (Fig. 1). Each group, containing from 1 to 100 dots, was generated with a liquid crystal based spatial light modulator (SLM) and 4*f* optical system. The holograms for the SLM were generated with an adapted weighted Gerchberg-Saxton (GSW) algorithm, which enabled discretized

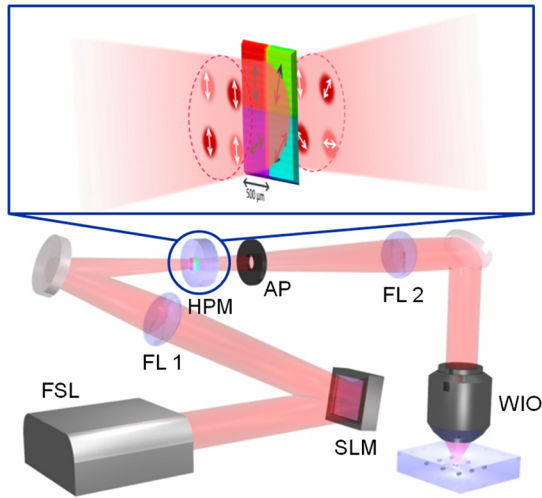


FIG. 1 (color online). 5D optical storage ultrafast writing setup: Femtosecond laser (FSL), Fourier lens (FL), aperture (AP) and water immersion objective (WIO) (1.2 NA). Linearly polarized (white arrows) beams with different intensity levels propagate simultaneously through each half-wave plate segment with different slow axis orientation (black arrows). The colors of the beams indicate different intensity levels.

multilevel intensity control [27,26]. The discretized multilevel intensity control enabled data multiplexing via retardance. By using the adapted GSW algorithm, several discrete levels of intensity could be achieved with a single hologram [26]. However, the algorithm controls only the relative ratio of different intensity levels. As the number of dots varies from one hologram to another, the absolute intensity of each spot varies. Thus, the corresponding intensity levels generated by different holograms are different and create fluctuations of the retardance value from one hologram to another. The problem is resolved by introducing a negative feedback loop into the algorithm, which redistributes the surplus of energy out of the modification region, fixing each intensity level generated by all holograms to the certain value (Fig. 2). The excess energy is blocked by an aperture (AP) placed after the half-wave plate matrix (HPM) (Fig. 1) and does not affect data recording.

The oriented slow axis is perpendicular to the polarization of the incident beam [20]. Hence, the azimuth of the slow axis can be controlled by the polarization of the incident beam, which is normally accomplished by rotating a half-wave plate. However, the rotation takes a relatively long time (>10 ms) and considerably reduces writing speed. To avoid this, a laser imprinted half-wave plate matrix (see half-wave plate matrix in Fig. 1), made of 4 segments, was added to the $4f$ optical system enabling motion free polarization control. In the focus plane of the first Fourier lens, where the half-wave plate matrix was placed, several beams with different intensity distribution were projected by the hologram displayed on the SLM.

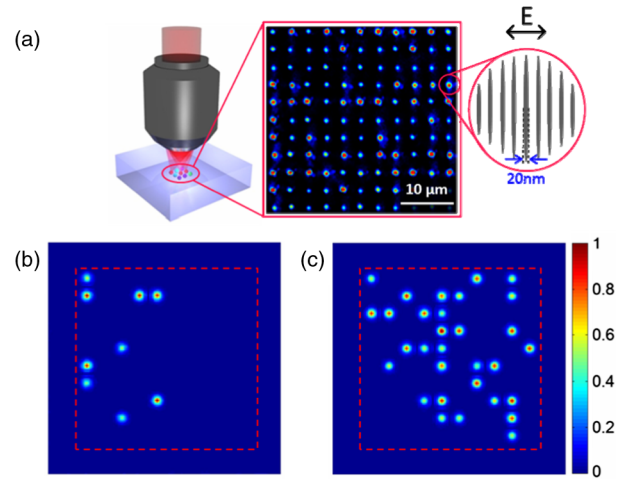


FIG. 2 (color online). Beam array multiple-level intensity control. (a) Schematic illustration of modification induced by a femtosecond laser. The colored dots indicate nanogratings induced by different intensity levels. (b)–(c) Two normalized intensity distributions calculated for two holograms from the adapted GSW algorithm. The area inside the red square is the modification region. The intensity distribution in (c) has more than 3 times the number of the multiple-level spots as compared to (b).

After passing through the segments of the half-wave plate matrix, beams with different polarizations were obtained. Subsequently, the plane of the half-wave plate matrix that contains predefined intensity and polarization distribution is reimaged directly into the sample by the microscope objective. After synchronizing the movement of the sample with the refresh rate of the SLM, multiple birefringent dots with four slow axis orientations and various phase retardance levels can be simultaneously imprinted (Supplemental Material, Movie 2) [26]. The information was encoded into two states of retardance and four states of slow axis orientation. Thus, each birefringent dot contained 3 bits of information.

The readout of the recorded information encoded in nanostructured glass was performed with a quantitative birefringence measurement system (Abrio, CRi Inc.) integrated into an optical microscope (BX51, Olympus Inc.). Light from a halogen lamp was circularly polarized and filtered with a bandpass filter (a central wavelength of 531 nm and a bandwidth of 30 nm). After being transmitted through the layers containing information, the signal was collected with a 0.6 NA objective and the state of polarization was characterized with a universal liquid crystal analyzer. The typical value of the retardance measured in the experiments was 40 nm. Using this system, we could easily resolve three birefringent layers separated by $20 \mu\text{m}$ in depth ([Fig. 3(a)] and Supplemental Material, Movie 1 [26]). The phase retardance [Fig. 3(c)] and slow axis orientation [Fig. 3(d)] were extracted from the raw data, then normalized [Figs. 3(e) and 3(f)] and discretized before the final result was achieved [Figs. 3(g) and 3(h)].

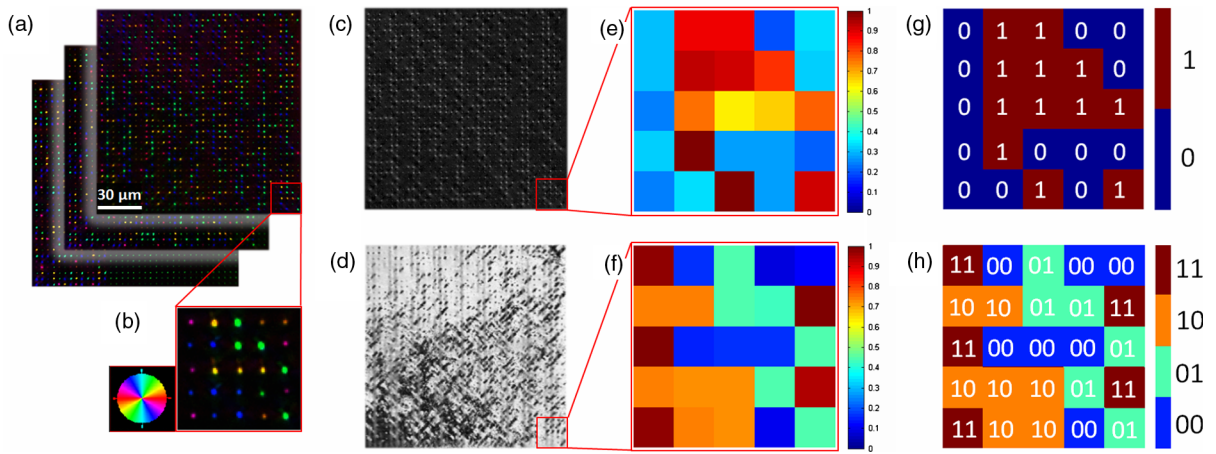


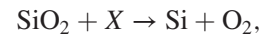
FIG. 3 (color online). 5D optical storage readout. (a) Birefringence measurement of the data record in three separate layers. (b) Enlarged 5×5 dots array. (c) Retardance distribution retrieved from the top data layer. (d) Slow axis distribution retrieved from the top data layer. (e),(f) Enlarged normalized retardance matrix and slow axis matrix from (b). (g),(h) Binary data retrieved from (e),(f).

The information was decoded by combining two binary data sets retrieved from the phase retardance and the slow axis orientation. Out of 11 664 bits, which were recorded in three layers, only 42 bit errors (bolded characters) were obtained (Table 1). Most of the errors were recurring and can be removed by additional calibration procedures, which accounts for the retardance dependence on polarization.

In the 5D optical storage shown in [Fig. 3(a)], the distance between two adjacent spots was $3.7 \mu\text{m}$ and the distance between each layer was $20 \mu\text{m}$. Applying the same writing method on a disc of conventional CD size with 60 layers, 18 GB capacity can be achieved. Using the same parameters we also successfully recorded across three layers a digital copy of a 310 KB file in PDF format [26].

The nanogratings are structural modifications which are known to exhibit high thermal and chemical durability. The nanogratings comprise of periodic assembly of nanoplanes with 20 nm thickness separated by about 300 nm and a negative index change of -0.2 , producing form birefringence (up to 10^{-2}) at the macroscopic scale. Close

investigation reveals that the refractive index of nanoplanes is reduced due to material porosity [24]. The formation of porous regions consisting of nanovoids filled with oxygen could be explained by the following mechanism: Femtosecond irradiation of silica glass produces self-trapped excitons with a lifetime of several microseconds. Recombination of self-trapped excitons is accompanied by generation of molecular oxygen due to the photosynthesis-like reaction,



where X denotes an exciton. The nanovoids could collapse with time leading to disappearance of the form birefringence of the modified region. Previous annealing experiments indicated that such modification can withstand at least 2 h of thermal annealing at 1000°C [23]. However, the accelerated aging measurements are required to evaluate the stability of nanogratings at room temperature and estimate the activation energy of the nanovoids collapse. The thermally activated decay time τ at the certain temperature T can be evaluated by Arrhenius law:

$$\frac{1}{\tau} = k = A \exp\left(-\frac{E_a}{k_B T}\right),$$

where k is the decay rate, E_a is the activation energy, A is the frequency factor, T is the absolute temperature, and k_B is the Boltzmann constant.

The decay rate was evaluated at several annealing temperatures in the range from 1173 to 1373 K, where measurable retardance change could be observed, by measuring the relative retardance decrease versus the annealing time (Fig. 4 inset). The experiment was performed with four different laser writing energies ($0.75\text{--}1.5 \mu\text{J}$). The variation of the relative retardance decrease for different energies was within 5%. The

TABLE I. Retrieved text from 5D memory.

The idea of the optical memory based on femtosecond laser writing in the bulk of transparent material was first proposed in 1996. More recently ultrafast laser writing of self-assembled nanogratings in class sa3 proposed for the polarization multiplexed optical memory, where the information encoding would be realized by means of two birefringence parameters, i.e. the slow axis orientation (4th dimension) and length of retardance (5th dimension), in addition to three spatial coordinates. The slow axis orientation and the retardance can be controlled by polarization and intensity of the incident beam respectively. The unprecedented parameters including 360 TB/disc data capacity, thermal stability up to 1000°C and practically unlimited lifetime. However the implementation of digital data storage, which is a crucial step towards the real world applications, has not been demonstrated by ultrafast laser writing. Here we successfully recorded and retrieved a digital copy of the text file in 5D using polarization controlled self-assembled ultrafast laser nanostructuring in silica glass.

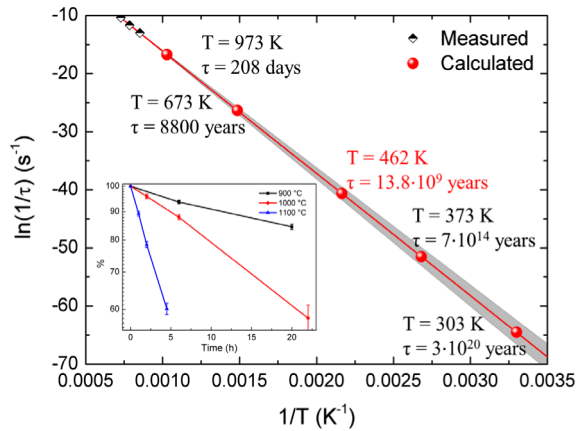


FIG. 4 (color online). Arrhenius plot of the nanogratings decay rate. Black dots indicate measured values; red dots are calculated based on the fitting results. The gray shaded zone indicates the tolerance of extrapolated values. At the temperature $T = 462$ K nanogratings would last for the current lifetime of the Universe. (Inset) The decay of the strength of retardance with time at different annealing temperatures.

birefringent structures (uniform squares 0.5×0.5 mm) used for these measurements were written with the same laser setup as described above. A relatively large area of the written structures was chosen to increase the precision and repeatability of retardance change measurements. From the obtained information, decay times at certain temperatures were evaluated and placed on the Arrhenius plot. The decay time at lower temperatures was easily extrapolated by a linear fit (Fig. 4). The best linear fit was obtained with activation energy of 1.81 ± 0.07 eV (thermal energy at room temperature is about 26 meV) and the frequency factor of 135 Hz. For comparison the activation energy measured in the erasure of the type I fiber Bragg gratings was 0.79–2.04 eV depending on the sample composition [28]. Assuming the scaling in Fig 4 holds at room temperature (303 K) the decay time of nanogratings is $3 \times 10^{20} \pm 1$ years, indicating unprecedented high stability of nanostructures imprinted in fused quartz. Even at elevated temperatures of $T = 462$ K, the extrapolated decay time is comparable with the age of the Universe—13.8 billion years. Obviously, extrapolation over such a long lifetime is not absolutely correct due to increasing error. Also it neglects the temperature variation over long periods of time, which cannot be easily evaluated. On the other hand, it is clear that if the temperature does not increase drastically, we would have an optical data storage with seemingly unlimited lifetime.

It can be affirmed that more states of polarization can be exploited for data encoding by fabricating a half-wave plate matrix with more than four segments. The number of intensity states can also be increased by changing the hologram generation parameters. Consequently, these added states, limited by the resolutions of the slow axis

orientation (4.7°) and the retardance (5 nm) [16], can enable more than one byte per modification spot with the current birefringence measurement system. By recording data with a 1.4 NA objective and shorter wavelength (250–350 nm), a disc with the capacity of 360 TB can be recorded [26]. Present errors (0.36% bit error rate for the .txt file recorded) have been investigated and found that the majority was repeatable. Therefore, with better calibration and signal processing techniques, the error rate can be significantly reduced.

The highest speed, which can be achieved with the current setup, is limited to 6 KB/s. The bottleneck of the data recording rate is created by the repetition rate (200 kHz) and the average power of the laser (6 W) and slow refresh rate of the SLM (60 Hz). We believe that 120 Mbit/sec data recording speed can be achieved by using a SLM with a faster refresh rate (20 kHz [29]) and high power ultrafast laser oscillators operating at megahertz repetition rates with an average power over 50 W [30]. The multiplexing technique can also help to exceed the data recording speed of the standard binary optical encoding system at the same laser repetition rate [26].

We finally note that the recording of a digital document into highly stable optical memory is a vital step towards an eternal archive [31]. Successful implementation of recording and readout of digital information unambiguously proves the viability of fused quartz as a high-density and, assuming the scaling of Arrhenius plot holds, long-lifetime storage medium. The advance from printing binary patterns to recording the first digital document is comparable to the leap from cave paintings to handwriting.

The work was supported by the project FEMTOPRINT, financed by the European Commission Factories of the Future program (FP7/ NMP/Project No. 260103), [32].

*Corresponding author.

jz2e11@soton.ac.uk

- [1] M. Hedstrom, *Comput. Humanit.* **31**, 189 (1997).
- [2] K. H. Lee, O. Slattery, R. Lu, X. Tang, and V. McCrary, *J. Res. Natl. Inst. Stand. Technol.* **107**, 93 (2002).
- [3] D. Eigler and E. Schweizer, *Nature (London)* **344**, 524 (1990).
- [4] G. E. Begtrup, W. Gannett, T. D. Yuzvinsky, V. H. Crespi, and A. Zettl, *Nano Lett.* **9**, 1835 (2009).
- [5] M. Irie and Y. Okino, *Jpn. J. Appl. Phys.* **45**, 1460 (2006).
- [6] O. Slattery, R. Lu, J. Zheng, F. Byers, and X. Tang, *J. Res. Natl. Inst. Stand. Technol.* **109**, 517 (2004).
- [7] Z. Sun, J. Zhou, and R. Ahuja, *Phys. Rev. Lett.* **98**, 055505 (2007).
- [8] J. H. Strickler and W. W. Webb, *Opt. Lett.* **16**, 1780 (1991).
- [9] E. N. Glezer, M. Milosavljevic, L. Huang, R. J. Finlay, T.-H. Her, J. P. Callan, and E. Mazur, *Opt. Lett.* **21**, 2023 (1996).
- [10] M. Watanabe and S. Juodkazis, *Appl. Phys. Lett.* **74**, 3957 (1999).

- [11] J. Squier and M. Müller, *Appl. Opt.* **38**, 5789 (1999).
- [12] A. Royon, K. Bourhis, M. Bellec, G. Papon, B. Bousquet, Y. Deshayes, T. Cardinal, and L. Canioni, *Adv. Mater.* **22**, 5282 (2010).
- [13] P. Zijlstra, J. W. M. Chon, and M. Gu, *Nature (London)* **459**, 410 (2009).
- [14] A. Podlipensky, A. Abdolvand, G. Seifert, and H. Graener, *Appl. Phys. A* **80**, 1647 (2005).
- [15] J. Heanue, M. Bashaw, and L. Hesselink, *Science* **265**, 749 (1994).
- [16] Y. Shimotsuma, M. Sakakura, P. G. Kazansky, M. Beresna, J. Qiu, K. Miura, and K. Hirao, *Adv. Mater.* **22**, 4039 (2010).
- [17] M. Beresna, M. Gecevičius, P. G. Kazansky, T. Taylor, and A. V. Kavokin, *Appl. Phys. Lett.* **101**, 053120 (2012).
- [18] C. Hnatovsky, V. Shvedov, W. Krolikowski, and A. Rode, *Phys. Rev. Lett.* **106**, 123901 (2011).
- [19] P. G. Kazansky, H. Inouye, T. Mitsuyu, K. Miura, J. Qiu, K. Hirao, and F. Starrost, *Phys. Rev. Lett.* **82**, 2199 (1999).
- [20] Y. Shimotsuma, P. G. Kazansky, J. Qiu, and K. Hirao, *Phys. Rev. Lett.* **91**, 247405 (2003).
- [21] V. R. Bhardwaj, E. Simova, P. P. Rajeev, C. Hnatovsky, R. S. Taylor, D. M. Rayner, and P. B. Corkum, *Phys. Rev. Lett.* **96**, 057404 (2006).
- [22] Y. Bellouard, A. Said, M. Dugan, and P. Bado, *Opt. Express* **12**, 2120 (2004).
- [23] E. Bricchi and P. G. Kazansky, *Appl. Phys. Lett.* **88**, 111119 (2006).
- [24] M. Lancry, B. Poumellec, J. Canning, K. Cook, J.-C. Poulin, and F. Brisset, *Laser Photonics Rev.* **7**, 953 (2013).
- [25] S. Richter, C. Miese, S. Döring, F. Zimmermann, M. J. Withford, A. Tünnermann, and S. Nolte, *Opt. Mater. Express* **3**, 1161 (2013).
- [26] See Supplemental Material at <http://link.aps.org/supplemental/10.1103/PhysRevLett.112.033901> for Hologram, writing procedure, capacity and writing speed.
- [27] R. Di Leonardo, F. Ianni, and G. Ruocco, *Opt. Express* **15**, 1913 (2007).
- [28] O. Deparis, C. Corbari, P. G. Kazansky, and K. Sakaguchi, *Appl. Phys. Lett.* **84**, 4857 (2004).
- [29] K.-i. Aoshima, N. Funabashi, K. Machida, Y. Miyamoto, K. Kuga, T. Ishibashi, N. Shimidzu, and F. Sato, *J. Disp. Technol.* **6**, 374 (2010).
- [30] S. V. Marchese, C. R. E. Baer, A. G. Engqvist, S. Hashimoto, D. J. H. C. Maas, M. Golling, T. Südmeyer, and U. Keller, *Opt. Express* **16**, 6397 (2008).
- [31] “The Long Now Foundation”, <http://longnow.org/about/> (2013).
- [32] <http://www.femtoprint.eu/>.